

## Tomography of Polars

Axel D. Schwope, Robert Schwarz, Andreas Staude

*Astrophysikalisches Institut Potsdam, Potsdam, Germany*

Claus Heerlein

*Institut für Theoretische Physik II, University Erlangen, Germany*

Keith Horne and Danny Steeghs

*Physics and Astronomy, University of St. Andrews, Scotland*

**Abstract.** We are reviewing the power of Doppler tomography for detailed investigations of polars (magnetic cataclysmic binaries without accretion disk). Using high-resolution spectroscopy in combination with tomography as analytic tool, the structure and extent of the accretion flows and accretion curtains in the binaries can be uncovered and the irradiated and non-irradiated parts of the mass-donating secondary stars can be made visible. In addition we show, how basic system parameters like the binary inclination and the mass ratio can be addressed by tomography.

### 1. Introduction

Doppler tomography of disk CVs has become fashionable about a decade ago by the pioneering study of Marsh & Horne (1988). It maps emission line regions by regarding an observed line profile as projection of the velocity field along the line of sight. While rotating the binary star delivers a set of projections in different directions as the line of sight rotates with respect to the line-emitting regions. Given time-resolved spectra  $f(v, \phi)$  with suitable resolution in radial velocity  $v$  and binary phase  $\phi$ , the 2-dimensional constraints from half a binary orbit suffice to construct a 2-dimensional map of the system in Doppler coordinates  $(v_x, v_y)$ . Orbital and streaming velocities both contribute to the observed Doppler profiles and make Doppler maps degenerate in that respect. Thus, a unique and straight transformation from Doppler space into real space is impossible. The interpretation of Doppler maps therefore requires additional modelling.

The first application of Doppler tomography to an AM Herculis star (polar), VV Pup, and a candidate AM Her star, GQ Mus, has been described by Diaz & Steiner (1994a, 1994b). These attempts, although undertaken with not very high spectral resolution, have shown the dramatic difference between Doppler maps of magnetic and non-magnetic cataclysmic binaries due to the presence of either accretion disks or accretion streams (e.g. Kaitchuck et al. 1994). Gas streams have been uncovered also for the first time by means of Doppler tomography in

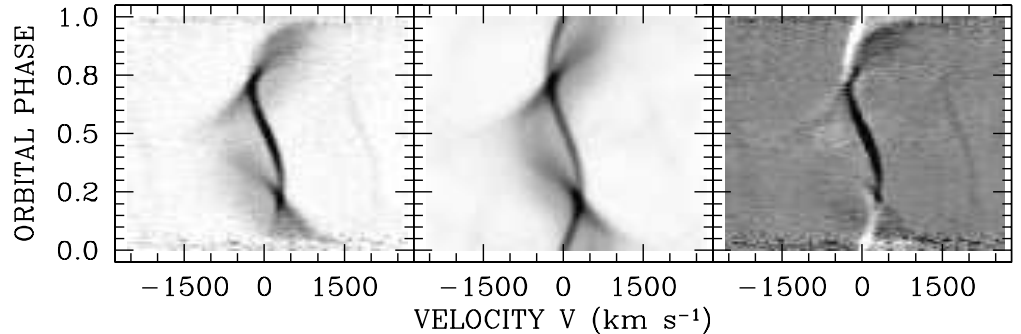


Figure 1. Trailed spectrogram of the He II emission line of HU Aqr observed in the 1993 high state (adapted from Schwöpe et al. 1997). The observed data has been transformed into Doppler space (Fig. 4) and projected again into the observers space (middle panel). The residuals between the two trails shown in the left and middle panels are shown right.

Algol systems by Richards et al. (1995). Deep insight into the unique, because bright and eclipsing, polar HU Aqr was possible through high-time resolution observations thus clearly revealing the presence of a ballistic accretion stream, an accretion curtain and a partially shielded secondary star.

In this article we describe recent progress made in this field through observations of several polars and the development of theoretical models.

## 2. Tomography and polars

Doppler tomography implicitly assumes that emission is completely optically thin and bound to the orbital plane of the binary. The latter condition requires that systemic velocities have been removed from the data. Both prerequisites are violated in polars due to the presence of optically thick radiating or absorbing surfaces and the presence of out-of-plane velocities along magnetic field lines and we shortly address the relevance of both effects for the interpretation of Doppler maps.

In Fig. 1 we show trailed spectrograms based on (a) observations of HU Aqr in its high accretion state, (b) projection of the Doppler map shown in Fig. 4, and (c) the difference between both. HU Aqr is an eclipsing polar with a prominent narrow emission line component (NEL) originating on the irradiated hemisphere of the secondary star. Due to the high inclination of the system this component is self-eclipsed by the star and visible only when the irradiated hemisphere is in view. The Doppler map is highly structured and allows a detailed view into the binary. It is nevertheless impossible by straightforward application of the tomographic inversion process to reach a good fit to the data (small  $\chi^2$ ) due to the self-eclipse of the NEL and the eclipse of the other emission components from the accretion stream by the mass-donating secondary star. This causes the

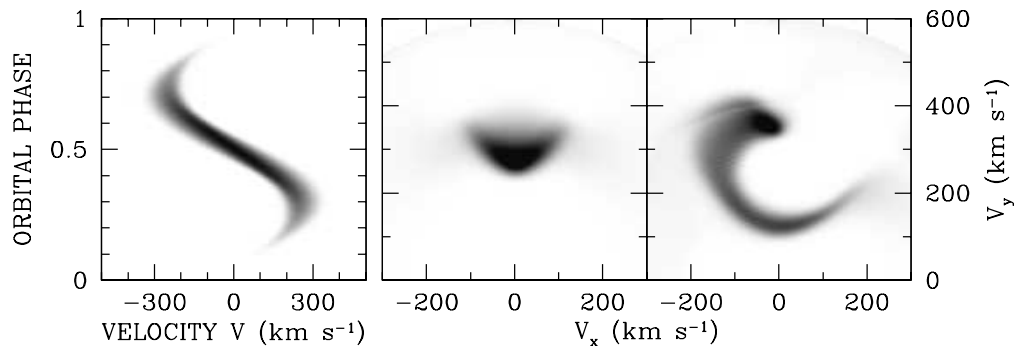


Figure 2. Numerical experiments demonstrating the influence of a non-zero systemic velocity. (*left*) Synthetic trailed spectrogram of an emission line originating on the Roche lobe of the secondary star irradiated by a point source at the white dwarf. (*middle*) Reconstructed Doppler map with the correct systemic velocity  $v_z = 0 \text{ km s}^{-1}$ . (*right*) Reconstruction with an assumed velocity  $v_z = 100 \text{ km s}^{-1}$ .

large systematic residuals of Fig. 1. Optical thick emission in the stream itself also violates one of the basic assumptions of tomography (but allows mapping of the observed brightness variation on a given surface, see the contribution by Vrielmann & Schwope in this volume). We mention three recipes which can be applied in order to improve on the goodness of fit: (a) use of different subsets of the data (in the optical thin case the data from half a binary orbit give a full map; one can construct a series of maps, using for each map half of the data,  $\Delta\phi = \phi_{\text{start}} + 0.5$ , sequentially shifting the start phase  $\phi_{\text{start}}$ , and inspect these series for systematic changes); (b) decomposition of the line profiles e.g. by removing the NEL from the secondary star; (c) mapping of the lines on predefined surfaces. Rutten & Dhillon (1994) have established with their ‘Roche tomography’ a first version of this kind. The more complicated (and much less well-defined) application to accretion streams and curtains is presently missing.

In order to demonstrate the effect of systemic velocities  $\gamma$  (or equivalently the effect of out-of-plane velocities) we show in Fig. 2 synthetic line profiles originating on the illuminated hemisphere of the secondary star (the NEL) and reconstructions with two different values of  $\gamma$ . The map with the correct value  $\gamma = 0 \text{ km s}^{-1}$  reconstructs the shape of the Roche lobe well (within the limits set by the assumed spectral resolution and optical thick emission). Reconstructions with  $v_z = \gamma \neq 0$  result in maps with arc-shaped or ring-like structures centred on the nominal position of emission with radius  $\sim\gamma$ . Hence, maps based on spectral data with large  $\gamma$ -velocities or large out-of-plane velocities may be significantly blurred. While one can of course correct for non-zero  $\gamma$ -velocities, emission at  $v_z \neq 0$  cannot be suppressed or removed from the data. However, the impact of this kind of emission on the maps can become large only for low-inclination systems but these are generally unfavourable targets for Doppler tomography due to their low projected radial velocities in the plane.

### 3. Basic binary parameters derived from Doppler maps

Fig. 3 compares trailed spectrograms and Doppler maps of the He II line at 4686 Å of the high-inclination, eclipsing system UZ For ( $P_{\text{orb}} = 126.5$  min) and of BL Hyi with binary period  $P_{\text{orb}} = 113.6$  min. The inclination of the latter system is debated.

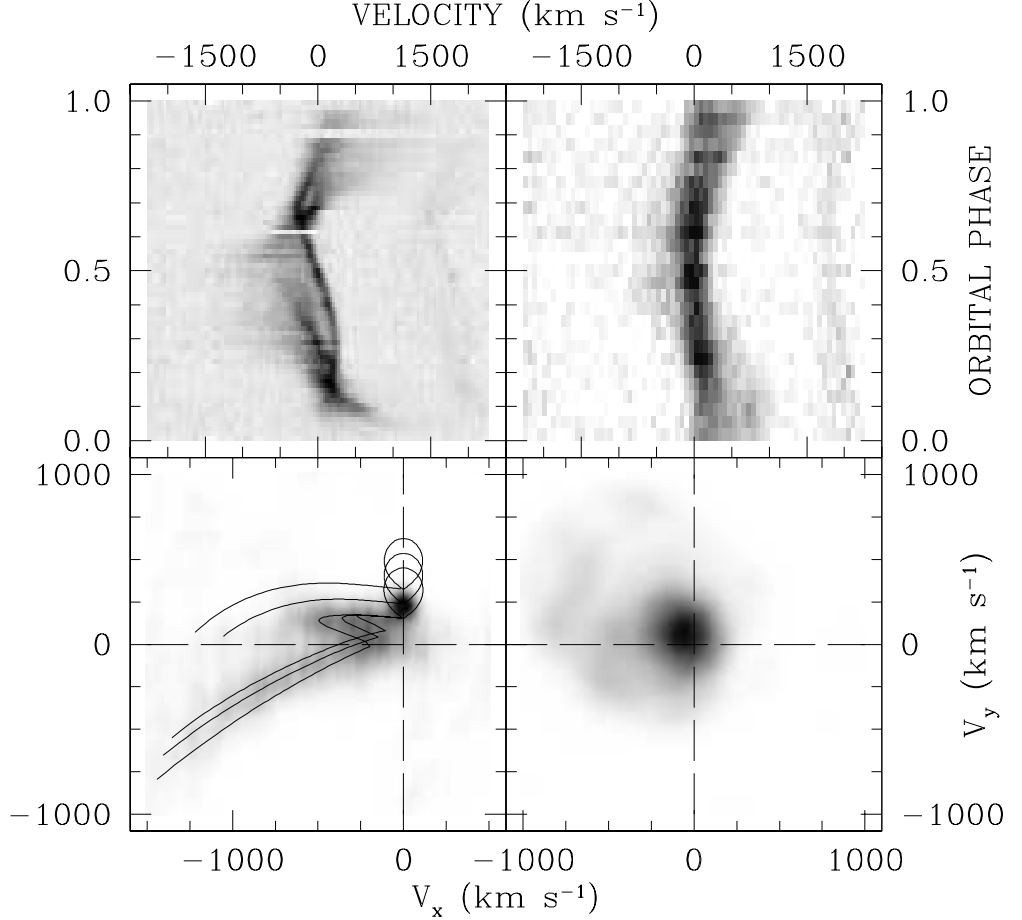


Figure 3. Trailed spectrograms (top) and Doppler maps (bottom) of the polars UZ For and BL Hyi of the emission line He II 4686 Å. The data of BL Hyi have only about half the spectral resolution than that of UZ For. The overlays in the lower left panel show Roche lobes of the secondary star and ballistic trajectories for mass ratios  $Q = 8, 5, 3$  from top to bottom, respectively.

The trailed spectrogram of UZ For shows several line components displaying pronounced radial velocity and intensity variations. In general, this behaviour is similar to that seen in the twin system HU Aqr at almost the same orbital period,  $P_{\text{orb}} = 125.0$  min (Fig. 1). The Doppler map clearly reveals three different

structures: (a) the irradiated hemisphere of the secondary as spot on the axis  $v_x = 0 \text{ km s}^{-1}$ , (b) the ballistic part of the accretion stream extending at nearly constant  $v_y$  from the secondary star down to  $v_x \simeq -600 \dots -700 \text{ km s}^{-1}$ , and (c) the magnetically dominated part of the stream which starts at about the origin and stretches into the lower left quadrant, becoming very dim at  $(v_x, v_y) \simeq (-1500, -700) \text{ km s}^{-1}$ . We refer to the ballistic part of the stream also as the horizontal stream, because it is assumed to be strictly bound to the orbital plane having no vertical velocity component  $v_z$ . If one assumes that the centre of light of the horizontal stream in the Doppler map follows a one-particle trajectory in the gravitational potential of the binary with mass ratio  $Q$  one has a good handle on the value of  $Q$ . However, Schwöpe, Mantel & Horne (1997) have shown that in the case of HU Aqr the horizontal stream in the map and the expected single-particle trajectory appear apart from each other (see Fig. 4). As shown below in Fig. 6, V1309 Ori seems to be another counterexample.

Another constraint on the mass ratio comes from the location of the bright spot on or near the irradiated surface of the secondary. Again, the location of the photocentre can be used to determine the size of the Roche lobe and hence the mass ratio  $Q$ . This approach assumes a certain relation between the velocities of the photocentre and the centre of mass and can be calculated with published irradiation models (Horne & Schneider 1989; Beuermann & Thomas 1990). In HU Aqr both methods yielded values of  $Q$  which were mutually exclusive and one had to compromise on an average value (see Fig. 4).

In UZ For both methods yield results which are in agreement with each other. Roche radii and ballistic trajectories for three different values of  $Q$  are overlaid on the Doppler map of UZ For ( $Q = M_{\text{wd}}/M_2 = 8, 5, 3$  from top to bottom). They show best agreement with both features, the ballistic stream and the illuminated portion of the secondary star for the lowest mass ratio assumed. This picture certainly excludes the high value of  $Q$  (and a high mass of the white dwarf) proposed by Beuermann, Thomas and Schwöpe (1988) based on low-resolution spectral observations of the Na-doublet from the secondary and is just compatible with the range of  $Q$ 's proposed by Bailey & Cropper (1991). Based on a photometric investigation of the eclipse light curve the latter authors derived  $Q = 5$ .

The Doppler map of UZ For also uncovers the location of the bulk of emission from the accretion stream. Assuming a certain orientation and strength of the (dipolar) magnetic field the motion of a test particle and its location in Doppler coordinates can be followed from the point  $L_1$  down close to the surface of the white dwarf (see Schwöpe et al. 1997 for a full description of the model). With a co-latitude of the magnetic axis  $\delta = 15^\circ \equiv 165^\circ$  and an azimuth  $\varphi = 45^\circ$  excellent agreement between the observed and modelled location of the stream can be reached. The three trajectories shown in Fig. 3 couple onto magnetic field lines  $\varphi = 10^\circ - 20^\circ$  prior to eclipse centre. These parameters predict a location of the accretion spot at co-latitude  $26^\circ (\equiv 154^\circ)$ , azimuth  $31^\circ$ , and, with the azimuth of the coupling region of about  $15^\circ$ , also the occurrence of an X-ray absorption dip at phase 0.96. The former value is in good agreement, the latter two disagree with the detailed modelling of extended EUVE-observations by Warren, Sirk & Vallergera (1995) who observed the dip at phase 0.91 and the spot at an azimuth of  $49^\circ$ . This leaves three possibilities open: (1) either our

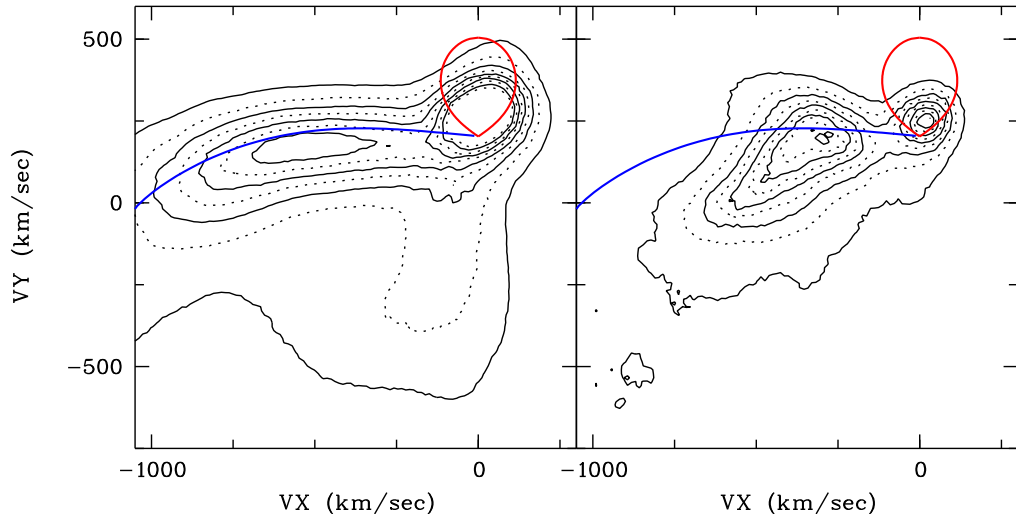


Figure 4. Doppler maps of the eclipsing polar HU Aqr in the light of the He II 4686 emission line observed in the 1993 high (left) and the 1996 reduced state of accretion (right). The overlays indicate the size of the Roche lobe of the secondary and the ballistic trajectory for a mass ratio  $Q = 4$ .

modelling is wrong, or (2) the stream that we are seeing in the Doppler maps feeds a secondary accretion spot which is different from that seen with EUVE and ROSAT, or (3) our map reveals a pronounced re-arrangement of the accretion geometry. Since we don't believe that (1) applies, a more careful analysis to be performed will discern between (2) and (3).

The determination of the binary inclination of polars has been the domain of polarimetrists for nearly two decades. In most cases different investigations yielded results agreeing with each other within about  $10\text{--}20^\circ$ . This is not true for BL Hya where Cropper (1987) and Pirola, Reiz & Coyne (1987) derived a high inclination close to eclipse,  $i \simeq 70^\circ$ , whereas Schwöpe & Beuermann (1989) arrived at  $i \simeq 30^\circ$ . The trailed spectrogram and the Doppler map shown in Fig. 3 suggest that BL Hya almost certainly has a low orbital inclination. Neither a NEL from the secondary star with corresponding high radial velocity amplitude sticks out nor do the velocities in the stream reach such high values as in UZ For or HU Aqr nor is a pronounced photometric variability of the line radiation recognizable. The Doppler map correspondingly is an unstructured mountain of light centred on some location where the stream and the secondary star are expected. The radial velocity curve of the emission lines observed in BL Hya reveals a velocity  $v_z \simeq 120 \text{ km s}^{-1}$  if the lines in individual spectra are fitted by single Gaussians. Hence, the blurring effect described in the previous section additionally smears the map.

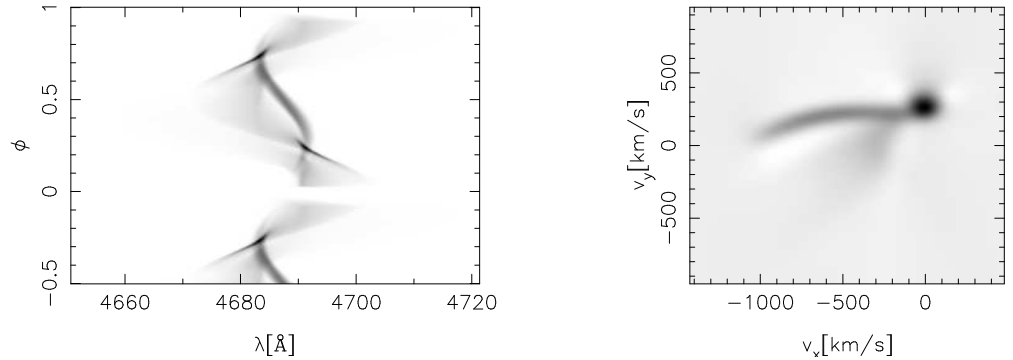


Figure 5. Simulated trailed spectrogram and Doppler map for HU Aqr in its high accretion state (Heerlein et al. 1998).

#### 4. HU Aqr: raising and lowering the accretion curtain

There is only one system which was observed with sufficient high spectral and time resolution in different accretion states allowing Doppler tomography, HU Aqr (Fig. 4, Schwöpe et al. 1997, 1998).

At both occasions the tomograms show an asymmetrically irradiated secondary star. Recombination radiation from the secondary is always centred at  $v_x > 0 \text{ km s}^{-1}$  which means that some kind of accretion curtain was always shielding the leading side of the star. The major difference between both maps concerns the emission from the accretion stream. In the high accretion state the stream penetrates the magnetosphere along the ballistic trajectory much deeper than at reduced accretion which seems to be obvious but nevertheless is directly confirmed by imaging of the stream for the first time. When coupling onto field lines the velocity vector of a plasma cell is assumed to be changing over a very short distance in real space. This leads to a jump of the stream in Doppler coordinates  $(v_x, v_y)$ . The stream 'turns sharper around the corner' in the high state which results in a larger jump towards the origin than in the low state. Hence the appearance of both parts of the stream in the Doppler map is affected by the change of the accretion rate. The one-particle ballistic trajectory plotted in Fig. 4 was computed for  $Q = 4$ . It does not coincide with the center of light of the observed ballistic stream but it represents the best compromise between estimates of  $Q$  based on the location of the ballistic stream and the NEL in the map. The reason for the displacement is not understood.

A further step towards a detailed understanding of the trailed spectra of polars in general but of HU Aqr in its high accretion state in particular has been undertaken recently by Heerlein, Horne & Schwöpe (1998). They developed a still quite simple stripping model for the accretion stream in three dimensions and considered radiation reprocessing in optically thick approximation from the ballistic stream and the accretion curtain connected to it. Irradiation of the companion star was included in their code but without shielding of the secondary by the curtain. The length of the ballistic stream, the size of and the veloci-

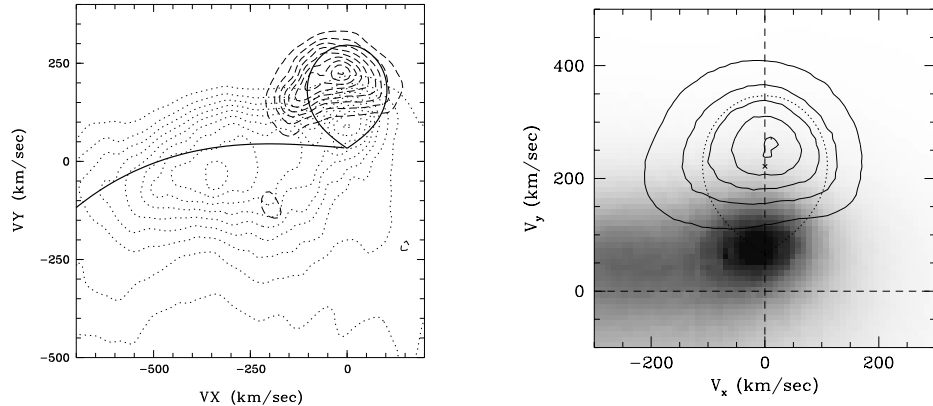


Figure 6. Combined Doppler maps of He II emission lines and Na I absorption lines of the long-period eclipsing polar V1309 Ori (left) and of QQ Vul (right). Overplotted are the Roche lobes of the secondary stars for mass ratios  $Q = 1.75$  and  $Q = 1.71$ , respectively. The maps of the Na I lines are shown as contour plots (dashed contours left, solid contours right), these lines are clearly visible only on the non-irradiated side of the companion stars.

ties in the curtain are depending on a few basic system parameters, mass ratio, accretion rate, orientation and strength of the magnetic field. By variation of either parameter the trailed spectra change, the predicted trailed spectrogram for the least-squares solution achieved by Heerlein et al. is reproduced in Fig. 5 together with the corresponding Doppler map. The images shown there should be compared with Figs. 1 and 4. The model reflects well the main observed features, it can, however, not explain the displacement of the horizontal stream. It also predicts a significantly better focussed ballistic stream than the observations show (the models were using the same spectral resolution as the data). A solution for the discrepancies lies probably in the details of the fragmentation of the stream, its more complex inner structure and a more complicated magnetic field topology.

Finally we would like to mention that in the low accretion state a significant amount of emission is seen in the upper left quadrant above the ballistic trajectory which is also not compatible with our current understanding of the streams in polars and suggestive of a complex flow pattern in the magnetosphere.

## 5. Irradiated companion stars

Fig. 6 compares the He II emission and Na I absorption lines of V1309 Ori and QQ Vul. In these long-period systems the secondary is big enough not to become outshone by the stream and the accretion spot even in their high accretion states. The Na I lines are originating in the photospheres of the mass-donating late-type stars. The He II emission from these secondaries originates from a quasi-chromosphere which is formed above the photosphere on response to the intensive EUV/X-ray irradiation from the hot spot on the white dwarf. The



luminosity of the irradiating source is higher than that of the exposed star and apart from possible partial shielding by an accretion curtain these stars are fully exposed.

To our knowledge there are no model calculations available in the literature which may be applied directly to this situation. The situation is similar to the HZ Her/Her X-1 system where several models with different level of sophistication has been developed (e.g., London et al. 1981) but the type of the irradiated star and of the irradiating source are clearly different here. Brett & Smith (1993) have developed a first model applicable to CVs irradiation by a moderately hot (17000 K) white dwarf in LTE. They took in favour of their approach King's (1989) argument that the ionizing radiation cannot reach the photosphere. Their model showed already that the temperature structure and the emitted spectrum of the irradiated star are changed markedly.

Our data clearly support this view Na I emission in QQ Vul and V1309 Ori is strongly suppressed if visible at all on the irradiated hemisphere. This seems to be the common picture in polars, other examples are AM Her (Davey & Smith 1992) and HU Aqr (unpublished data from the authors) and tells us that all attempts to determine the stellar masses (in particular  $M_{\text{wd}}$ ) by radial velocity measurements of the secondary stars have to pay attention to this distortion. The detection of the irradiation distortion requires high resolution spectroscopy (dispersion and time) of faint absorption lines in a spectral region which is highly contaminated by night sky emission and atmospheric absorption lines and is, therefore, an ambitious observational task.

## 6. Conclusions and outlook

Doppler tomography of polars has become possible in recent years through the mounting of sensitive low-noise detectors in high-resolution spectrographs at 4m-class telescopes. The angular resolution thus achieved is of the order of *micro arcsec*. Images of accretion streams, accretion curtains and the two sides of X-ray illuminated M-stars could be gained. Interpretation of these Doppler images has just started and opens the field for a physical understanding and modelling of the accretion plasma between the two stars. We mention a few topics for future work in that direction: (1) The width of the ballistic plasma streams and their (occasionally) displaced location with respect to a one-particle trajectory are not matched by purely kinematical considerations. Turbulence and MHD effects obviously have to be taken into account (although this will be difficult to achieve in practice due to the complexity of the problem). (2) When modelling the emission from the stream/curtain region in this paper we have made use mainly of the velocity information. Future work should address also the line intensities (in different line components, in different species) and try to derive the temperature/ionization structure by application of photoionization models. (3) The secondary stars provide a natural laboratory for the application of so-called next generation stellar models (NGSM, e.g., Hauschildt, Baron & Allard 1997) taking into account irradiation by the hot spot on the white dwarf. Again, this is not an easy and straightforward task due to NLTE and the anisotropy but models and observations are approaching a state where this kind of research becomes feasible.

Finally, our view into these type of binaries can be sharpened by utilization of future 8m telescopes, e.g. the VLT UT2 with UVES. We will be able then to look e.g. for starspots on the secondary stars by means of Doppler imaging and thus be able to address the question if giant starspots might be responsible for the low states in cataclysmic binaries.

**Acknowledgments.** This work has been supported through DLR grants 50 OR 9403 5 and 50 OR 9706 8 and by the DFG grant Schw 536/8-1.

## References

- Bailey, J., Cropper, M., 1991, MNRAS 253, 27  
Beuermann, K., Thomas, H.-C., 1990, A&A 230, 326  
Beuermann, K., Thomas, H.-C., Schwope, A.D., 1988, A&A 195, L15  
Brett, J.M., Smith, R.C., 1993, MNRAS 264, 641  
Cropper, M., 1987, MNRAS 228, 389  
Davey, S., Smith, R.C., 1992, MNRAS 257, 476  
Diaz, M.P., Steiner, J.E., 1994a, A&A 283, 508  
Diaz, M.P., Steiner, J.E., 1994b, ApJ 425, 252  
Hauschildt, P.H., Baron, E., Allard, F., 1997, ApJ 483, 390  
Heerlein, C., Horne, K., Schwope, A.D., 1998, MNRAS, in press  
Horne, K., Schneider, D.Q., 1989, ApJ 343, 888  
Marsh, T.R., Horne, K., 1988, MNRAS 235, 269  
Kaitchuk, R.H., Schlegel, E.M., Honeycutt, R.K., et al., 1994, ApJS 93, 519  
King, A.R., 1989, MNRAS 241, 365  
London, R., McCray, R., Auer, L.H., 1981, ApJ 243, 970  
Piirola, V., Reiz, A., Coyne, G.V., 1987, A&A 185, 189  
Richards, M.T., Albright, G.E., Bowles, L.M., 1995, ApJ 438, L103  
Rutten, R.G.M., Dhillon, V.S., 1994, A&A 288, 773  
Schwope, A.D., Beuermann, K., 1989, A&A 222, 132  
Schwope, A.D., Mantel, K.-H., Horne, K., 1997, A&A 319, 894  
Schwope, A.D., et al., 1998, In: Wild Stars in the Old West, eds. S. Howell et al., ASP Conf. Ser. 137, pp. 44  
Warren, J.K., Sirk, M.M., Vallergera, J.V., 1995, ApJ 445, 909